Online Size Exclusion Chromatography-Fast Photochemical Oxidation of Proteins Allows for Targeted Structural Analysis of Conformationally Heterogeneous Mixtures

Surendar Tadi[1] and Joshua S. Sharp[1,2]*

[1]Department of BioMolecular Sciences, University of Mississippi, Oxford, MS, 38677, United States
[2]Department of Chemistry and Biochemistry, University of Mississippi, Oxford, MS 38677, United States
[*]To Whom Correspondence Should Be Addressed:

Joshua Sharp
Department of BioMolecular Sciences
445 Faser Hall
University, MS 38677
jsharp@olemiss.edu

Structural analysis of proteins in a conformationally heterogeneous mixture has long been a difficult problem in structural biology, resulting in complex challenges in data analysis or complete failure of the method. In structural analysis by covalent labeling mass spectrometry, conformational heterogeneity will result in data reflecting a weighted average of all conformers, greatly complicating data analysis and potentially causing misinterpretation of results. Here, we describe a method coupling size exclusion chromatography in an HPLC format with Hydroxyl Radical Protein Footprinting (HRPF) using online Fast Photochemical Oxidation of Proteins (FPOP). Using controlled mixtures of myoglobin and apomyoglobin as a model system to allow for controllable conformational heterogeneity, we demonstrate that we can obtain HRPF footprints of both holomyoglobin and apomyoglobin as they elute off of the SEC column. Comparison of online SEC-FPOP data of both mixture components with traditional FPOP data of each individual component shows that we can obtain the exact same footprinting pattern for each conformation in an online format with real-time FPOP. Using this method, conformations within conformationally heterogeneous mixtures can now be individually probed by SEC-FPOP, and the stability of the FPOP label allows this structural information to be retained.

Introduction

Hydroxyl radical protein footprinting (HRPF) is a method for probing the topography of proteins in solution. A protein of interest is exposed to hydroxyl radicals freely diffusing in solution. The radicals are very short-lived, very highly reactive, and rapidly oxidize amino acid side chains present on the surface of the folded protein. The apparent rate of oxidation is primarily a function of two factors: **(1)** the inherent chemical reactivity of the amino acid side chain [1,2] and **(2)** the exposure of the side chain to the hydroxyl radical, which correlates directly with solvent accessible surface area [3-5]. Information about the topography of the folded protein is frozen in this chemical "snapshot" of the protein surface, after which the protein can be processed (e.g. deglycosylated, extracted from lipid membranes, proteolytically digested, etc.) and analyzed by liquid chromatography coupled to mass spectrometry (LC-MS). By comparing the signal intensity from an unoxidized peptide versus all oxidized forms of that peptide, the apparent rate of oxidation for a particular peptide can be determined [4,6,7]. HRPF is typically used to compare the same (or very closely related) amino acid sequence in two or more conformations, or three-dimensional shapes. In such experiments, the inherent reactivity of a given amino acid side chain does not differ between samples, so changes in the apparent reactivity of an amino acid side chain due to hydroxyl radicals can be directly correlated with changes in the solvent accessible surface area.

The broad reactivity of the hydroxyl radical probe, the ability to decouple the probe chemistry from the analytical technology (allowing for sample processing), and the broad applicability of LC-MS technology have enabled HRPF to fill an important niche in probing biological systems that have proven difficult to approach with standard high-resolution structural technologies such as multidimensional NMR and X-ray crystallography. Systems where HRPF has found success in probing protein structure and protein interactions include membrane proteins [8-14], protein oligomerization and aggregation processes [15-17], and binding interfaces between proteins and unpurified complex mixtures of ligands [18].

What many of these difficult biological systems have in common is the presence of more than a single structure in solution to probe, which we will refer to here as conformational heterogeneity. Conformationally heterogeneous systems have the unfortunate distinction of

being both difficult to analyze with modern techniques as well as areas of intense interest due to an emerging understanding of their importance in biology and biochemistry. Standard high-resolution structural technologies have difficulties with conformational heterogeneity, as the presence of multiple major conformations can prevent protein crystallization, dampen signals in both crystallography and NMR, and make data very difficult to interpret. Conformational heterogeneity can arise from a single protein that samples multiple conformers in solution, post-translational modifications (PTMs) resulting in conformational changes, prosthetic groups, chemical modifications, co-existing sequence variants, or oligomerization and aggregation processes where the thermodynamics of protein aggregation and disaggregation results in a distribution of multimeric structures with topographies differing based on the number and arrangement of subunits. In each case of conformational heterogeneity, multiple topographies of the same protein sequence exist simultaneously in solution, with each topography playing an important role in the observed function (or dysfunction, as the case may be) of the protein. While in some cases these conformationally heterogeneous samples can be separated chromatographically, if the heterogeneity is dynamic (e.g. aggregation processes), the sample may not remain conformationally homogeneous long enough for structural interrogation.

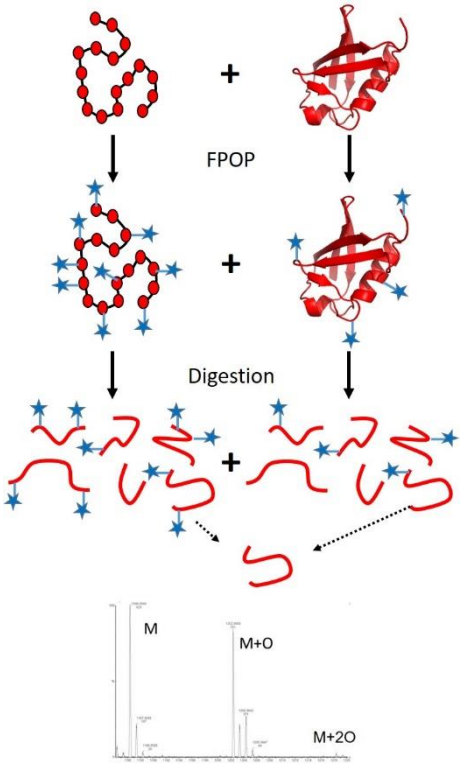

Figure 1. HRPF Fails to Capture Individual Conformations. A protein coexisting in two conformations (left: unfolded, right: folded) is subjected to FPOP, which labels the more "open" conformation more thoroughly. However, after proteolytic digestion of the oxidized proteins, the contribution of each conformer cannot be deconvoluted. Only an average topography, which does not accurately represent either conformation, can be determined.

In conformationally heterogeneous samples, current HRPF approaches yield data that represents an *average* of all conformers in solution. An illustration of the modern HRPF process as applied to a conformationally heterogeneous sample is shown in **Figure 1**. Briefly,

samples are exposed to a sub-microsecond burst of hydroxyl radicals generated by the laser-induced photolysis of hydrogen peroxide in a process termed Fast Photochemical Oxidation of Proteins (FPOP) [19]. The hydroxyl radicals are consumed faster than large conformational changes occur, with the vast majority of the radical reacted in under one microsecond [20,21], although resulting protein-centered radicals are longer-lived [20,22]. Hydroxyl radicals oxidize amino acid side chains available on the surface in molecules in both **conformation A** and **conformation B**, with each side chain having a rate constant that is dependent upon the accessibility of that side chain in that protein conformation to the radical. This results in two separate chemical "snapshots" of protein structure being taken—a snapshot of proteins in **conformation A** and a distinct snapshot of proteins in **conformation B** when the radical burst was formed.

At this point, the radical footprints are distinct and identifiable based on the overall amount of oxidation of the protein—proteins in a more compact conformation will have fewer average oxidation events per molecule than those in a more open conformation, and can be differentiated in the mass spectrum of the intact protein [23]. However, the next step in modern HRPF is a proteolytic digestion of the protein mixture into modified peptides. After this step, it is no longer possible to differentiate peptides that were linked with **conformation A** from those that were linked with **conformation B**—all modified peptides are mixed together and can no longer be attributed to their parent conformation. Therefore, the solvent accessibility reported for a given amino acid is an *average* of the solvent accessibility of that amino acid in **conformation A** and **conformation B** weighted by the fraction of the protein in each conformation; the HRPF data do not accurately represent either conformation.

In this manuscript, we describe the development of online HPLC-FPOP labeling using size exclusion chromatography (SEC) to separate a synthetic conformationally heterogeneous mixture of myoglobin and apomyoglobin and an online FPOP system to label the separated conformers as they elute off of the column. A post-column micro-tee is used to introduce the FPOP mixture without HPLC pump or column contamination. Using adenine radical dosimetry [24], we are able to ensure comparable radical exposure of both components of the mixture. Using this method, we can generate HRPF footprints of each conformer in the mixture that are

statistically indistinguishable from those obtained using traditional FPOP on each conformer individually. This method now allows FPOP to generate HRPF data for individual conformers within conformationally heterogeneous mixtures, expanding our ability to structurally interrogate these challenging, yet biologically crucial targets.

EXPERIMENTAL SECTION.

Materials. Apomyoglobin, myoglobin, catalase, glutamine formic acid, hydrochloric acid, sodium phosphate, and 2-(Nmorpholino)-ethanesulfonic acid (MES) were obtained from Sigma-Aldrich (St. Louis, MO). Adenine and LCMS-grade acetonitrile and water were purchased from Fisher Scientific (Fair Lawn, NJ). Hydrogen peroxide (30%) was purchased from J. T. Baker (Phillipsburg, NJ). Fused silica capillary was purchased from Molex, LLC (Lisle, IL). Sequencing grade modified trypsin was obtained from Promega (Madison, WI)

Online FPOP. A mixture of myoglobin and apomyoglobin at a concentration of 5 mg/mL of each protein was loaded on an ACQUITY UPLC Protein BEH SEC, 150mm, 125 Å, 1.7 µm (Waters Milford, MA) using the autosampler and capillary pumps of a Dionex Ultimate Nano 3000 (Dionex, Sunnyvale, CA). Separation of proteins was performed with an isocratic gradient of 100 mM sodium phosphate (pH 6.8) at flow rate of 30 µL/min for 60min. Column eluant flowed through a Dionex UV detector, where protein elution was detected by UV absorbance at 280 nm. A Peek microtee (Upchurch Scientific) mixer was installed immediately after the UV detector, with one inlet port leading to the SEC column, one inlet port to the FPOP reagent, and the outlet port to the 100 µm ID, 365 µm OD fused silica capillary for laser exposure. FPOP reagent was mixed 1:1 with the eluant using a Legato 101 syringe pump (KD Scientific, Holliston, MA) with a gastight syringe (Hamilton, Reno, NV), to a final concentration of 100 mM hydrogen peroxide, 16 mM glutamine, and 2 mM adenine. After the mixing tee, sample was flowed through the focused beam path of a COMPex Pro 102 KrF excimer laser (Coherent Inc., Santa Clara, CA) focused to a fluence of ~13 mJ/mm^2 pulsing at 20 Hz to generate hydroxyl radicals with a 15% exclusion volume. Sample collection was determined by detection of eluting protein by UV absoruance at 280 nm; 35-45 minutes for myoglobin and 65-75 minutes for apomyoglobin. Samples were collected immediately after illumination into vials containing 120µL of a quench solution of 0.5 µg/µL methionine amide and 0.2 µg/µL catalase to eliminate secondary oxidation. After

quenching, the absorbance of the adenine dosimeter at 265 nm was measured using a Nanodrop UV/Vis spectrophotometer [24]. Samples were processed for LC-MS as described below.

Offline FPOP: All samples were prepared and analyzed in triplicate. A final concentration of 5mg/mL each of myoglobin of apomyoglobin was mixed with final concentration of 50mM sodium phosphate (pH 7.4), 1mM of adenine, 17mM glutamine and 2uM hydrogen peroxide was added just before laser exposer loaded on gastight syringe (Hamilton, Reno, NV). The mixture was flowed through the focused beam path of the excimer laser pulsing at 20 Hz, with an exclusion volume 15% and a fluence of ~13 $mJ/mm^{2\cdot}$ Exposed sample was collected into vials containing 0.3ug/ul of catalase and 0.5 µg/mL of methionine amide [25,26]. Samples were incubated at room temperature for 30min and adenine readings were recorded with an average difference in absorbance at 265 nm of 0.10. Samples were processed for LC-MS analysis as described below.

LC-MS Analysis. 50 mM Tris, pH 8.0 and 1 mM $CaCl_2$ was added to samples after online FPOP. The samples were incubated at 90 °C for 15 min to denature the protein. After denaturation, samples were cooled to room temperature and a 1:20 trypsin/protein weight ratio was added to the samples for overnight digestion at 37 °C with sample rotation. Digestion was terminated by heating the samples to 95 °C for 10 min. The protein and peptide samples were loaded on to an Acclaim PepMap 100 C18 nanocolumn (0.75 mm × 150 mm, 2 µm, Thermo Fisher Scientific). Separation of peptides on the chromatographic system was performed using mobile phase A (0.1% formic acid in water) and mobile phase. B (0.1% formic acid in acetonitrile) at a flow rate of 300 nL/min. The peptides were eluted with a gradient consisting of 2 to 35% solvent B over 22 min, ramped to 95% solvent B over 5 min, held for 3 min, and then returned to 2% solvent B over 3 min and held for 9 min [27]. Peptides were eluted directly into the nanospray source of an Orbitrap Fusion instrument controlled with Xcalibur version 2.0.7 (Thermo Fisher, San Jose, CA) using a conductive nanospray emitter (Thermo Scientific). All data were acquired in positive ion mode. The spray voltage was set to 2300 V, and capillary temperature was set to 300 °C. In CID mode, full MS scans were acquired from m/z 350 to 2000 followed by eight subsequent MS/MS scans on the top eight most abundant peptide ions.

Online HRPF Analysis. Data acquired by LC-MS and LC-MS/MS of oxidized and unoxidized peaks were initially identified by Byonic version v2.10.5 (Protein Metrics, San Carlos, CA) and validated manually. Unoxidized and oxidized peptide peaks were quantified by integration of the selected ion chromatogram peaks of unoxidized and oxidized peptides plus one or more oxygen atoms (mass error = 10 ppm), with all resolved oxidation isomers summed using Xcalibur. Oxidation events per peptide were calculated using eq 1

$$n_{OX} = [\, I\,(+16)\text{ oxidized} \times 1 + I\,(+32)\text{ oxidized} \times 2 + I\,(+48)\text{oxidized} \times 3 + \ldots] \;/\; [I\text{ unoxidized} + I\,(+16)\text{ oxidized} + I\,(+32)\text{oxidized} + I\,(+48)\text{oxidized}\ldots] \quad (1)$$

Oxidation events at peptide level were denotes as n_{OX} and peak intensities of oxidized and unoxidized were denoted as I [27]. All major identified oxidation products are the net addition of one or more oxygen atoms.

RESULTS AND DISCUSSION

SEC separation of myoglobin and apomyoglobin. In order to prevent interference from vastly changing radical scavenging backgrounds, as well as to preserve native protein conformation during separation, an isocratic method for separating our two conformers (apomyoglobin and myoglobin) was developed. We used an aqueous buffer system using sodium phosphate buffer, a relatively unreactive inorganic buffer that is often used for preserving native structure. An outline for our method for LC-FPOP is shown in **Figure 2**.

We developed a method for the isocratic aqueous separation of apomyoglobin and myoglobin using SEC chromatography. The column gave negligible background with a blank injection at 280

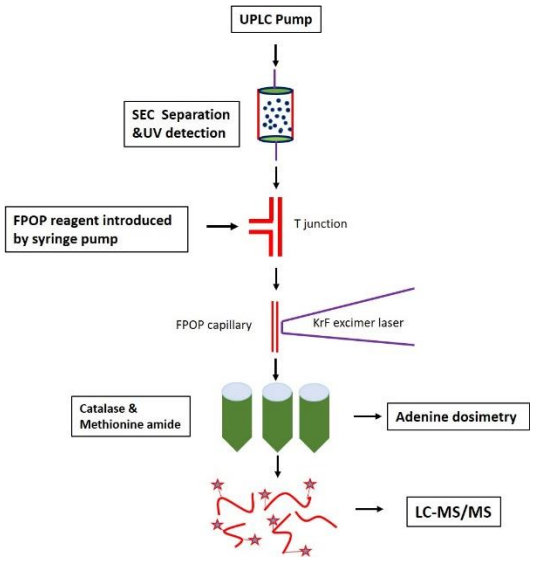

Figure 2. Schematic of Online FPOP: Protein mixture was separated on LC-SEC chromatography and FPOP reagent is injected with T junction after protein separation. Separated protein mixed with FPOP reagent was exposed to laser. Collected in a vial consist of quench solution.

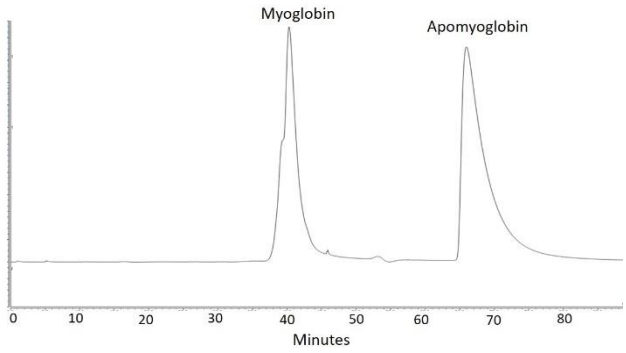

Figure 3. SEC separation of a 1:1 mixture of myoglobin and apomyoglobin with UV detection at 280 nm.

nm (**Figure S1**, Supporting Information). Injection of pure myoglobin gives one major peak that elutes at 44 minutes, while injection of pure apomyoglobin gives one major peak at 65 minutes (**Figure S2**, Supporting Information). SEC separation of a synthetic 1:1 mixture of myoglobin and apomyoglobin was easily achieved under these conditions, as shown in **Figure 3**. The baseline resolution of myoglobin and apomyoglobin makes for simple chromatographic differentiation between the two conformers.

Comparison of Online LC-FPOP and Traditional Offline FPOP. The compatibility of LC pump components and the SEC column to hydrogen peroxide is unclear. Additionally, UV illumination in the UV detector for detection of eluting protein will photoactivate the hydrogen peroxide, making the production and labeling of artifactual conformations likely. Therefore, we split in solvent components for FPOP post-UV detector. A mixture of 2x concentrated FPOP reagent (hydrogen peroxide, adenine dosimeter, and glutamine radical scavenger) was introduced with micro tee after the column and UV detector, but prior to flow intersection with the excimer laser beam path. Sample corresponding to myoglobin and apomyoglobin were collected from 35 to 45min and 65 to 75 min respectively, quenched separately immediately after FPOP. Adenine dosimetry was used to ensure that samples were exposed to equivalent radical doses [24,28]. The results from online LC-FPOP of a 1:1 mixture of myoglobin and apomyoglobin were compared with traditional offline FPOP to determine if online LC-FPOP generated comparable results from a mixture of products.

Results from LC-FPOP and traditional off-line FPOP were remarkably consistent with one another. Almost identical sequence coverage was obtained from samples, regardless of if FPOP was performed online on the mixture, or offiline (**Figure S3** through **Figure S6**, Supporting Information). Similarly, almost identical product distributions were obtained by online LC-FPOP of the mixture and offline FPOP of the pure conformer. An example is shown in **Figure 4**, an

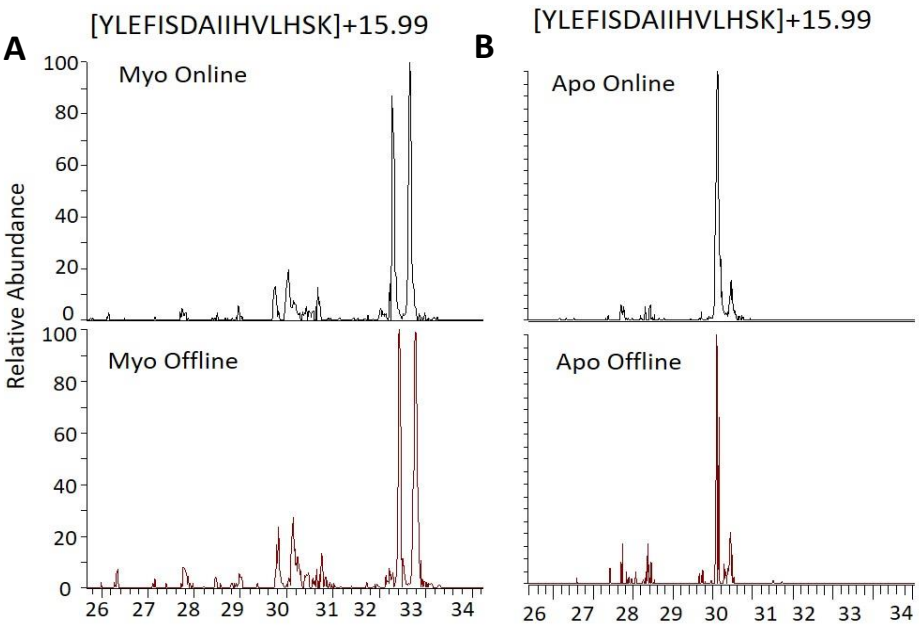

Figure 4. Comparison of the extracted ion chromatogram of the +16 Da oxidation products of peptide 103-118 from **(A)** myoglobin and **(B)** apomyoglobin. In each subfigure, the top panel is from online LC-FPOP of a 1:1 mixture, while the bottom panel is from traditional FPOP of the pure protein conformer.

extracted ion chromatogram of the +16 Da oxidation products of the 103-118 peptide that shows clear conformational differences between apomyoglobin and holomyoglobin. The LC trace shows a highly similar profile and relative quantity of oxidation products between the online LC-FPOP of the mixture, and offline FPOP of the pure conformer, while both online and traditional methods generate very different oxidation profiles between apomyoglobin and holomyoglobin. These data indicate that LC-FPOP of a mixture allows the researcher to obtain equivalent topographical information as traditional offline FPOP of the pure conformer.

The equivalency of topographical information obtained by LC-FPOP of a mixture of conformers compared with traditional FPOP of pure conformers is also obvious in a more global view as shown in **Figures 5** and **6**. Both online LC-FPOP of the mixture of conformers and offline FPOP of the pure conformers showed obvious differences in topography in regions impacted by heme binding. Close examination reveals that no statistically significant differences for any peptide can be identified between online LC-FPOP of the mixture and traditional FPOP of the pure conformer for myoglobin (**Figure 5**) or apomyoglobin (**Figure 6**).

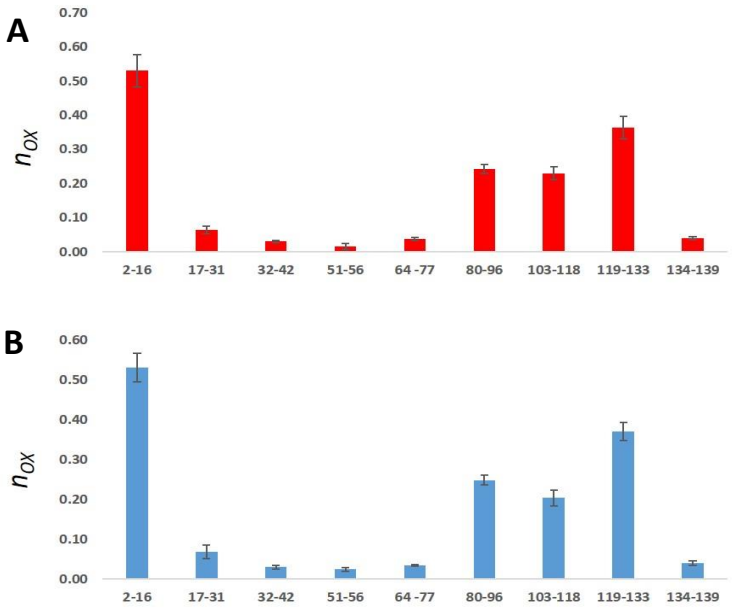

Figure 6. Comparison of myoglobin peptide oxidation between **(A)** online FPOP of a 1:1 myoglobin:apomyoglobin mixture and **(B)** offline FPOP of pure myoglobin. Error bars represent one standard deviation from a triplicate data set. No statistically significant differences in oxidation were detected between online and offline data ($\alpha = 0.05$).

CONCLUSION

Here, we demonstrate the use of online LC-FPOP to probe protein topography of a synthetic mixture of two conformers, with results that are indistinguishable from traditional FPOP analysis of either pure conformer. We targeted conformers that are non-dynamic (apomyoglobin vs. holomyoglobin) to ensure proper control of conformer composition in our synthetic mixture. The ability to structurally differentiate non-dynamic conformers from a mixture is very powerful and convenient, especially for the structural characterization of complex analytes like disulfide bond shuffling products[29] and misfolded proteins[30]. However, LC-FPOP will also work for dynamic conformer mixtures so long as the dynamics are slower than the chromatographic separation timescale so the conformers can separate on the column. These mixtures include a surprisingly broad array of biomedically important systems that are currently subjects of intense investigation, such as monoclonal antibody aggregation[31], oligomerization of amyloids such as tau[32], protein-polysaccharide complexes[33] and slow-

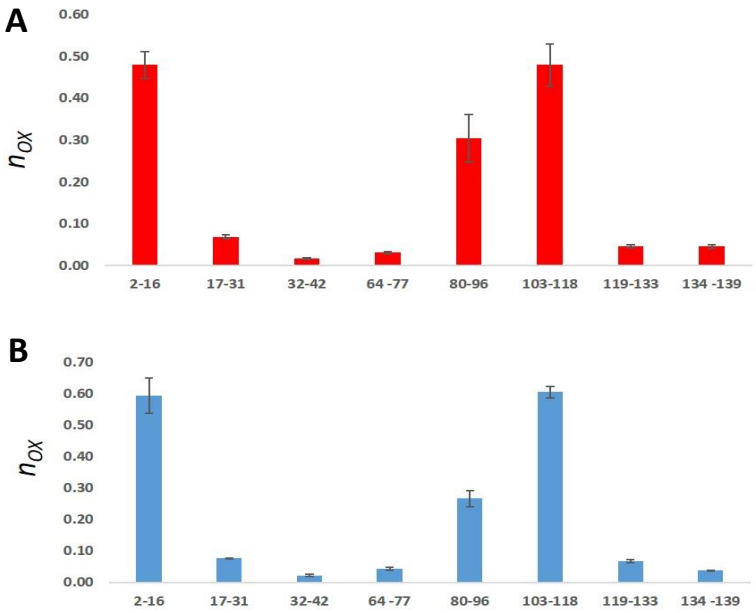

Figure 7. Comparison of apomyoglobin peptide oxidation between **(A)** online FPOP of a 1:1 myoglobin:apomyoglobin mixture and **(B)** offline FPOP of pure apomyoglobin. Error bars represent one standard deviation from a triplicate data set. No statistically significant differences in oxidation were detected between online and offline data ($\alpha = 0.05$).

exchanging conformers in intrinsically disordered proteins[34]. Given the problems that exist in the structural probing of these systems currently, LC-FPOP represents a significant new tool for enabling structural investigations.

We demonstrate LC-FPOP using SEC in order to achieve separation using an isocratic gradient with aqueous buffer. The LC-FPOP technology is not limited to SEC; any chromatography that uses an isocratic gradient could potentially be used for LC-FPOP so long as the buffer system is compatible with FPOP. An isocratic gradient is convenient in order to minimize changes in the hydroxyl radical scavenging capacity of the solvent. However, with the recent report of inline hydroxyl radical dosimetry[35], binary solvent systems can be designed with matched radical scavenging capacities for aqueous separations (for example, a binary gradient of sodium formate/sodium chloride for strong anion exchange chromatography)[1] and tested in real time for suitability. The ability to couple inline radical dosimetry with a method for real-time control of hydroxyl radical generation would allow for real-time scavenging compensation[28], providing even more flexibility in LC gradient design. As the use of adsorptive

stationary phases and faster separation times would allow for probing of dynamic systems with more subtle changes in conformation and faster kinetics of conformational change, we are pursuing these advances in current studies.

Acknowledgements: This work was supported by the National Science Foundation (1608685) and the National Institute of General Medical Sciences (R01GM127267).

Conflict of Interest Disclosure

J.S.S. discloses a significant financial interest in GenNext Technologies, Inc., a small company seeking to commercialize technologies for protein higher order structure analysis.

References

(1) Buxton, G. V.; Greenstock, C. L.; Helman, W. P.; Ross, A. B. *Journal of Physical and Chemical Reference Data* **1988**, *17*, 513-886.
(2) Xu, G.; Chance, M. R. *Anal Chem* **2005**, *77*, 4549-4555.
(3) Chance, M. R. *Biochem Biophys Res Commun* **2001**, *287*, 614-621.
(4) Charvatova, O.; Foley, B. L.; Bern, M. W.; Sharp, J. S.; Orlando, R.; Woods, R. J. *J Am Soc Mass Spectrom* **2008**, *19*, 1692-1705.
(5) Huang, W.; Ravikumar, K. M.; Chance, M. R.; Yang, S. *Biophys J* **2015**, *108*, 107-115.
(6) Guan, J. Q.; Vorobiev, S.; Almo, S. C.; Chance, M. R. *Biochemistry* **2002**, *41*, 5765-5775.
(7) Sharp, J. S.; Tomer, K. B. *Biophys J* **2007**, *92*, 1682-1692.
(8) Gupta, S.; Chai, J.; Cheng, J.; D'Mello, R.; Chance, M. R.; Fu, D. *Nature* **2014**, *512*, 101-104.
(9) Konermann, L.; Pan, Y. *Expert Rev Proteomics* **2012**, *9*, 497-504.
(10) Pan, Y.; Brown, L.; Konermann, L. *J Am Soc Mass Spectrom* **2010**, *21*, 1947-1956.
(11) Orban, T.; Gupta, S.; Palczewski, K.; Chance, M. R. *Biochemistry* **2010**, *49*, 827-834.
(12) Pan, Y.; Stocks, B. B.; Brown, L.; Konermann, L. *Anal Chem* **2009**, *81*, 28-35.
(13) Angel, T. E.; Gupta, S.; Jastrzebska, B.; Palczewski, K.; Chance, M. R. *Proc Natl Acad Sci U S A* **2009**, *106*, 14367-14372.
(14) Smedley, J. G.; Sharp, J. S.; Kuhn, J. F.; Tomer, K. B. *Biochemistry* **2008**, *47*, 10694-10704.
(15) Wang, X.; Watson, C.; Sharp, J. S.; Handel, T. M.; Prestegard, J. H. *Structure* **2011**, *19*, 1138-1148.
(16) Gau, B.; Garai, K.; Frieden, C.; Gross, M. L. *Biochemistry* **2011**, *50*, 8117-8126.
(17) Kiselar, J. G.; Datt, M.; Chance, M. R.; Weiss, M. A. *J Biol Chem* **2011**, *286*, 43710-43716.
(18) Li, Z.; Moniz, H.; Wang, S.; Ramiah, A.; Zhang, F.; Moremen, K. W.; Linhardt, R. J.; Sharp, J. S. *J Biol Chem* **2015**, *290*, 10729-10740.
(19) Hambly, D. M.; Gross, M. L. *J Am Soc Mass Spectrom* **2005**, *16*, 2057-2063.
(20) Watson, C.; Janik, I.; Zhuang, T.; Charvatova, O.; Woods, R. J.; Sharp, J. S. *Anal Chem* **2009**, *81*, 2496-2505.
(21) Gau, B. C.; Sharp, J. S.; Rempel, D. L.; Gross, M. L. *Anal Chem* **2009**, *81*, 6563-6571.
(22) Vahidi, S.; Konermann, L. *J Am Soc Mass Spectrom* **2016**, *27*, 1156-1164.
(23) Venkatesh, S.; Tomer, K. B.; Sharp, J. S. *Rapid Commun Mass Spectrom* **2007**, *21*, 3927-3936.
(24) Xie, B.; Sharp, J. S. *Anal Chem* **2015**, *87*, 10719-10723.
(25) Misra, S. K.; Orlando, R.; Weinberger, S. R.; Sharp, J. S. *The AAPS journal* **2019**, *21*, 019-0358.
(26) Riaz, M.; Misra, S. K.; Sharp, J. S. *Anal Biochem* **2018**, *562*, 32-36.
(27) Sharp, J. S.; Misra, S. K.; Persoff, J. J.; Egan, R. W.; Weinberger, S. R. *Analytical Chemistry* **2018**, *90*, 12625-12630.
(28) Misra, S. K.; Orlando, R.; Weinberger, S. R.; Sharp, J. S. *AAPS J* **2019**, *21*, 87.
(29) Wecksler, A. T.; Yin, J.; Lee Tao, P.; Kabakoff, B.; Sreedhara, A.; Deperalta, G. *Mol Pharm* **2018**, *15*, 1598-1606.
(30) Hu, Y.; Chen, S.; Xu, M.; Zhang, S. *Biotechnol Appl Biochem* **2004**, *40*, 89-94.
(31) Paul, A. J.; Schwab, K.; Hesse, F. *BMC Biotechnol* **2014**, *14*, 99.
(32) Mirbaha, H.; Holmes, B. B.; Sanders, D. W.; Bieschke, J.; Diamond, M. I. *J Biol Chem* **2015**, *290*, 14893-14903.
(33) Wu, F.; Dong, K.; Zhu, M.; Zhang, Q.; Xie, B.; Li, D.; Gan, H.; Linhardt, R. J.; Zhang, Z. *J Pharm Biomed Anal* **2019**, *164*, 668-671.
(34) Uversky, V. N. *Methods Mol Biol* **2012**, *896*, 179-194.
(35) Sharp, J. S.; Misra, S. K.; Persoff, J. J.; Egan, R. W.; Weinberger, S. R. *Anal Chem* **2018**, *90*, 12625-12630.